

# Nucleon superfluidity vs observations of cooling neutron stars

A. D. Kaminker<sup>1</sup>, P. Haensel<sup>2</sup>, and D. G. Yakovlev<sup>1</sup>

<sup>1</sup> Ioffe Physical Technical Institute, Politekhnicheskaya 26, 194021 St. Petersburg, Russia

<sup>2</sup> N. Copernicus Astronomical Center, Bartycka 18, 00-716 Warsaw, Poland

*kam@astro.ioffe.rssi.ru, haensel@camk.edu.pl, yak@astro.ioffe.rssi.ru*

Received x xxx 2001 / Accepted x xxx 2001

**Abstract.** Cooling simulations of neutron stars (NSs) are performed assuming that stellar cores consist of neutrons, protons and electrons and using realistic density profiles of superfluid critical temperatures  $T_{\text{cn}}(\rho)$  and  $T_{\text{cp}}(\rho)$  of neutrons and protons. Taking a suitable profile of  $T_{\text{cp}}(\rho)$  with maximum  $\sim 5 \times 10^9$  K one can obtain smooth transition from slow to rapid cooling with increasing stellar mass. Adopting the same profile one can explain the majority of observations of thermal emission from isolated middle-aged NSs by cooling of NSs with different masses either with no neutron superfluidity in the cores or with a weak superfluidity,  $T_{\text{cn}} < 10^8$  K. The required masses range from  $\sim 1.2 M_{\odot}$  for (young and hot) RX J0822–43 and (old and warm) PSR 1055–52 and RX J1856–3754 to  $\approx 1.45 M_{\odot}$  for the (rather cold) Geminga and Vela pulsars. Observations constrain the  $T_{\text{cn}}(\rho)$  and  $T_{\text{cp}}(\rho)$  profiles with respect to the threshold density of direct Urca process and maximum central density of NSs.

**Key words.** Stars: neutron – dense matter

## 1. Introduction

In recent years, great progress has been made in observations of thermal radiation from middle-aged isolated NSs. Main observational results are summarized in Fig. 1 which shows error bars of the effective surface temperature,  $T_{\text{s}}^{\infty}$ , as measured by a distant observer, versus stellar age  $t$  for eight sources. The youngest three are radio-quiet NSs in supernova remnants, the oldest is also a radio-quiet NS, while the others manifest themselves as radio pulsars. NS ages are mainly pulsar spindown ages or the estimated supernova ages. The age of the Vela pulsar is taken according to Lyne et al. (1996), and the age of RX J185635–3756 ( $\lg t$  [yr] = 5.95) is taken according to Walter (2001). The values of  $T_{\text{s}}^{\infty}$  come from the following sources: RX J0822–43 — Zavlin et al. (1999), 1E 1207–52 — Zavlin et al. (1998), RX J0002+62 — Zavlin & Pavlov (1999), PSR 0833–45 (Vela) — Pavlov et al. (2001), PSR 0656+14 — Possenti et al. (1996), PSR 0630+178 (Geminga) — Halpern & Wang (1997), PSR 1055–52 — Ögelman (1995), and RX J1856–3754 — Walter (2001). For all the sources but the Vela pulsar and RX J1856–3754 these data are presented in Table 3 in Yakovlev et al. (1999). For the Vela pulsar  $T_{\text{s}}^{\infty} = 0.68 \pm 0.03$  MK at  $1\sigma$  confidence level. For RX J1856–3754 we take  $T_{\text{s}}^{\infty} = 0.57 \pm 0.06$  MK (the central value is mentioned by Walter; we supplement it with an estimated error for a joint fit of the optical plus X-ray data). The values of  $T_{\text{s}}^{\infty}$  for the four youngest sources are

obtained from the observed X-ray spectra using hydrogen atmosphere models. They are more consistent with other information on these sources (distances, hydrogen column densities, inferred neutron star radii, etc) than the blackbody model of NS radiation. On the contrary, the blackbody model is more consistent for older sources, and we present the blackbody values of  $T_{\text{s}}^{\infty}$  for the older sources. We do not present observational data for some other sources. For instance, we do not consider a possible NS candidate in Cas A (e.g., Pavlov et al. 2000) because its nature is not clear.

We will interpret the observational data with the models of cooling NS. NSs of age  $t \lesssim 10^6$  yr are known to cool mainly via neutrino emission from their interiors, while the older NSs cool mainly via photon emission from the surface. We use our fully relativistic nonisothermal cooling code constructed by O. Gnedin and described in Gnedin et al. (2001). We employ the simplest NS models assuming that the NS cores consist of neutrons (n), protons (p) and electrons. We adopt a moderately stiff equation of state (EOS) of this matter proposed by Prakash et al. (1988) (their model I with the compression modulus of saturated nuclear matter  $K = 240$  MeV). Other physics input is the same as described in Gnedin et al. (2001). In particular, we place the core-crust interface at  $\rho = 1.5 \times 10^{14}$  g cm<sup>-3</sup>. The outer heat blanketing NS envelope is assumed to be made of iron (although the atmosphere may contain light elements) neglecting the effects of surface magnetic fields; the relation between  $T_{\text{s}}$  and the internal

NS temperature is taken from Potekhin et al. (1997). The validity of such approach is discussed, e.g., by Yakovlev et al. (1999). The maximum mass of our NS models is  $M_{\max} = 1.977 M_{\odot}$  (with the radius of 10.754 km) and the maximum central density is  $\rho_{c,\max} = 2.575 \times 10^{15} \text{ g cm}^{-3}$ . For the given EOS, powerful direct Urca process of neutrino emission (Lattimer et al. 1991) is forbidden at  $M < M_{\text{D}} = 1.358 M_{\odot}$  ( $\rho_{\text{c}} < \rho_{\text{D}} = 7.851 \times 10^{14} \text{ g cm}^{-3}$ ). If so, a NS undergoes a *slow* cooling mainly via modified Urca process of neutrino emission. A NS with  $M > M_{\text{D}}$  possesses a central kernel, where direct Urca process is open ( $\rho > \rho_{\text{D}}$ ); its cooling is *fast*.

The values of  $T_{\text{s}}^{\infty}$  for 1E 1207–52, RX J0002+62, and PSR 0656+14 may be consistent with slow cooling of non-superfluid NSs. RX J0822–43, PSR 1055-52 and RX J1856–3754 are too hot for slow cooling of a non-superfluid NS with the heat-blanketing envelope made of iron (although RX J0822–43 is consistent with the blanketing envelope made of light elements, Potekhin et al. 1997). The lower values of  $T_{\text{s}}^{\infty}$ , especially for the Vela and Geminga pulsars, are intermediate between slow and fast cooling of non-superfluid NSs. In non-superfluid NSs, the transition from slow to fast cooling with increasing  $M$  occurs in a very narrow mass range  $1 < M/M_{\text{D}} \lesssim 1.003$  (e.g., Page & Applegate 1992, Yakovlev et al. 2001). In principle, one can explain the Geminga and Vela data by cooling of non-superfluid NSs but the probability that NS masses fall in this very narrow mass range is too low to accept such explanation.

We will show that the observational data in Fig. 1 can be explained by the models of NSs with superfluid cores.

## 2. Nucleon superfluidity

We adopt traditional assumption that neutrons undergo singlet-state Cooper pairing in the NS crust and triplet-state pairing in the core, while protons undergo singlet-state pairing in the core. Microscopic calculations of the critical temperatures of the neutron and proton superfluidities (SFs),  $T_{\text{cn}}$  and  $T_{\text{cp}}$ , depend sensitively on the model of nucleon-nucleon interaction and many-body theory employed (see, e.g., Yakovlev et al. 1999, for references). All models predict pronounced density dependence of  $T_{\text{cn}}$  and  $T_{\text{cp}}$ . In particular,  $T_{\text{cn}}(\rho)$  for the singlet-state neutron SF has maximum at subnuclear densities in the crust and vanishes at  $\rho \sim 2 \times 10^{14} \text{ g cm}^{-3}$  while  $T_{\text{cn}}(\rho)$  for the triplet-state neutron SF grows up at subnuclear density, reaches maximum at  $\rho = (2 - 3) \rho_0$  ( $\rho_0 = 2.8 \times 10^{14} \text{ g cm}^{-3}$  is the saturation density of nuclear matter) and decreases with  $\rho$ , vanishing at  $\rho \sim (3 - 5) \times 10^{15} \text{ g cm}^{-3}$ .  $T_{\text{cp}}$  also has maximum at several  $\rho_0$  and vanishes at higher  $\rho$ . At  $\rho \sim (2 - 3) \rho_0$  the proton SF is typically stronger than the neutron one. SF of n and p reduces the emissivity of neutrino reactions and affects heat capacity of n and p. Moreover, SF initiates a specific neutrino emission associated with Cooper pairing of nucleons (Flowers et al. 1976). In this way nucleon SF becomes a strong regulator

of NS cooling. The appropriate physics input is described in Yakovlev et al. (2001).

SF of neutrons in the crust affects cooling of young NSs ( $t \lesssim 100 \text{ yr}$ ), in which the internal thermal relaxation is not over, and it does not affect cooling of middle-aged NSs we are interested in. To be specific, we neglect neutron SF in the crust. As for  $T_{\text{cn}}(\rho)$  and  $T_{\text{cp}}(\rho)$  in the NS core, we will not rely on any particular microscopic model but will try to find the models consistent with the observations. We parameterize the dependence of  $T_{\text{cN}}$  on the nucleon (N=n or p) wavenumber  $k = k_{\text{FN}} = (3\pi^2 n_{\text{N}})^{1/3}$  (measured in  $\text{fm}^{-1}$ ) as

$$T_{\text{cN}} = T_0 \frac{(k - k_0)^2}{(k - k_0)^2 + k_1^2} \frac{(k - k_2)^2}{(k - k_2)^2 + k_3^2}, \quad (1)$$

for  $k_0 < k < k_2$ , and  $T_{\text{cN}} = 0$  for  $k \leq k_0$  and  $k \geq k_2$ ,  $T_0$ ,  $k_0, \dots, k_3$  being free parameters.  $T_0$  regulates maximum of  $T_{\text{cN}}(\rho)$ ,  $k_0$  and  $k_2$  determine low-density and high-density  $T_{\text{cN}}(\rho)$  cutoffs, while  $k_1$  and  $k_3$  govern the shape of  $T_{\text{cN}}(\rho)$ . Let us present also our simple fit of the density dependence of the nucleon number density  $n_{\text{N}}$  (in  $\text{fm}^{-3}$ ) for the given EOS:

$$n_{\text{N}} = a \rho_{14}^b / (1 + c \rho_{14} + d \rho_{14}^2), \quad (2)$$

where  $\rho_{14} \equiv \rho / (10^{14} \text{ g cm}^{-3})$ ;  $a = 0.1675$ ,  $b = 1.8185$ ,  $c = 2.0288$ ,  $d = 0.02444$  for N=n, and  $a = 0.0006823$ ,  $b = 2.6767$ ,  $c = 0.1946$ ,  $d = 0.01604$  for N=p.

At the first step we neglect neutron SF in the core and adopt  $T_{\text{cp}}(\rho)$  displayed in Fig. 2. It is given by Eqs. (1) and (2) with  $T_0 = 2.029 \times 10^{10} \text{ K}$ ,  $k_0 = 0$ ,  $k_1 = 1.117 \text{ fm}^{-1}$ ,  $k_2 = 1.241 \text{ fm}^{-1}$ ,  $k_3 = 0.1473 \text{ fm}^{-1}$ . The maximum  $T_{\text{cp}} = 6.78 \times 10^9 \text{ K}$  takes place at  $\rho = 5.74 \times 10^{14} \text{ g cm}^{-3}$  and  $T_{\text{cp}}$  vanishes at  $\rho = 9.55 \times 10^{14} \text{ g cm}^{-3}$ . This proton SF is constructed artificially but is typical for SFs provided by microscopic calculations. In a not too massive NS ( $M \lesssim 1.45 M_{\odot}$ ,  $T_{\text{cp}}(\rho_{\text{c}}) \gtrsim 10^9 \text{ K}$ ) it will appear at the initial stage of NS cooling ( $t \lesssim 100 \text{ yr}$ ). Accordingly, the peak of neutrino emission due to Cooper pairing of p will take place at this early stage making almost no affect on the cooling curves (solid lines). Moreover, the internal temperature of the middle-aged NS will be much lower than  $T_{\text{cp}}$ . The proton SF will switch off the proton heat capacity and it will strongly suppress neutrino reactions involving protons, particularly, modified and direct Urca processes. However, the total heat capacity is mainly provided by neutrons being almost unaffected by proton SF.

The upper cooling curve is for the  $1.3 M_{\odot}$  NS (with the radius of 13.04 km) but it would be exactly the same for all  $M$  from  $M_{\text{D}}$  down to  $\sim 1.1 M_{\odot}$  (similar insensitivity to  $M$  is discussed, e.g., in Yakovlev et al. 1999). For  $t \sim (10^2 - 10^5) \text{ yr}$  this cooling curve goes noticeably higher than in a non-superfluid NS since SF suppresses neutrino emission and slows cooling of such a NS. This allows us to explain high surface temperature of RX J0822-43 by cooling of a superfluid NS with the heat blanketing envelope made of iron. Similar to the nonsuperfluid NS models, we have faster cooling at  $M > M_{\text{D}}$ . However, the SF

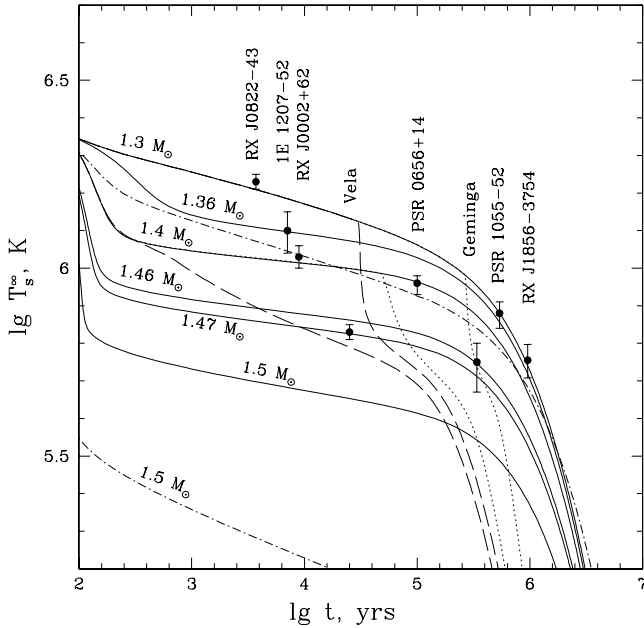


**Fig. 1.** Observational data (error bars) on surface temperatures of eight NSs (see the text) as compared with theoretical cooling curves obtained for proton and neutron SFs from Fig. 2. All cooling curves (except dot-and-dashed ones) are calculated for the same proton SF. Solid lines – no neutron SF for NS models with masses (from top to bottom) 1.3, 1.36, 1.4, 1.46, 1.47, and 1.5  $M_{\odot}$ . Dashed lines and dotted lines correspond to neutron SFs for  $M = 1.3$  and 1.4  $M_{\odot}$ . Dashed-and-dot lines are for non-superfluid 1.3  $M_{\odot}$  and 1.5  $M_{\odot}$  NSs.

suppression of neutrino emission strongly smoothes transition from slow to fast cooling and allows us to explain the low temperatures  $T_s^{\infty}$  of the Vela and Geminga pulsars by cooling of NSs with  $M \approx 1.47 M_{\odot}$ . With further increase of  $M$  to  $M_{\max}$  we obtain almost the same fast-cooling curves as in the absence of SF. These results are not sensitive to the specific choice of  $T_{cp}(\rho)$  near the maximum (at  $\rho \lesssim \rho_D$ ) as long as  $T_{cp}(\rho)$  is high (say,  $\gtrsim 3 \times 10^9$  K) for  $\rho \lesssim \rho_D$ . However, the transition from slow to fast cooling with increasing  $M$  is very sensitive to the decreasing slope of  $T_{cn}(\rho)$  at higher  $\rho$ . By shifting this slope to higher  $\rho$  we would obtain higher masses of the Vela and Geminga pulsars.

Our next step is to discuss the effects of neutron SF. Following the results of microscopic calculations we assume that this SF is generally weaker than the proton one in the NS core. If  $T_{cn} \lesssim 3.5 \times 10^8$  K, this SF appears in the NS core at  $t \gtrsim 100$  yr (for  $M \lesssim 1.45 M_{\odot}$ ). The NS core is then isothermal, and the temperature decreases uniformly over the core in the course of cooling. Thus the SF appears first in a spherical layer at those values of  $\rho = \rho_{CP}$  which correspond to maximum of  $T_{cn}(\rho)$ ,  $T_{cn}(\rho_{CP}) = T_{cn}^{\max}$ . Before that time the cooling curves are exactly the same (solid lines in Fig. 1) as in the absence of neutron SF. Once the neutron SF is switched on,

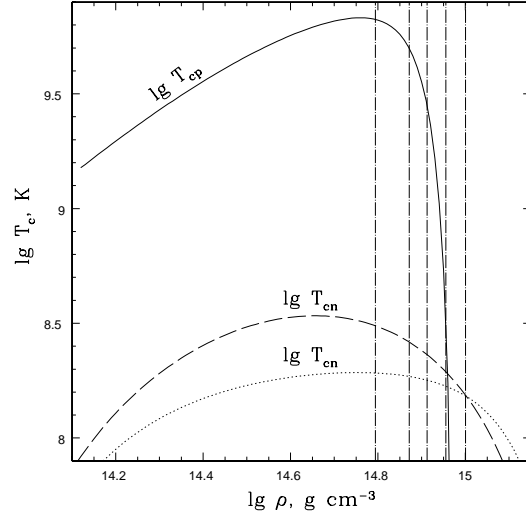


**Fig. 2.** Density dependence for one model of the proton critical temperature (solid line) and two models of neutron critical temperatures (dots and dashes) used in cooling simulations (Fig. 1). Vertical dot-and-dashed lines show the central densities of 1.1, 1.3, 1.4, 1.5 and 1.6  $M_{\odot}$  NSs.

powerful neutrino emission due to Cooper pairing of neutrons starts to operate. If  $\rho_{CP}$  is noticeably lower than the NS central density one can calculate the neutrino luminosity  $L_{CP}$  due to this Cooper pairing semianalytically. Its temperature dependence can be written as  $L_{CP}(T) = L_0 l(\tau)$ , where  $L_0$  is a normalization constant (which depends on  $T_{cn}(\rho)$  and NS model) while  $l(\tau)$  is a universal function of  $\tau = T/T_{cn}^{\max}$  (with  $l \propto (1 - \tau)^{3/2}$  at  $(1 - \tau) \ll 1$ ;  $l \propto \tau^8$  at  $\tau \ll 1$ , and with maximum at  $\tau \approx 0.795$ ). This neutrino emission cools the star very quickly producing sharp breaks of the cooling curves. The breaks are especially pronounced if the neutron SF appears at  $t \sim 10^4 - 10^6$  yr. Soon after the break onsets the cooling curves become even steeper due to reduction of the neutron heat capacity at  $T \ll T_{cn}$  and due to transition to photon cooling stage. The effect is illustrated in Fig. 1 which shows cooling curves (dots and dashes) for two models of neutron SF (dots and dashes) displayed in Fig. 2 and parameterized by Eqs. (1) and (2). In both cases  $k_0 = 1 \text{ fm}^{-1}$ . The dotted line in Fig. 2 corresponds to the following set of parameters:  $T_0 = 2.915 \times 10^8$  K,  $k_1 = 0.5664 \text{ fm}^{-1}$ ,  $k_2 = 2.767 \text{ fm}^{-1}$ ,  $k_3 = 0.2965 \text{ fm}^{-1}$ . Accordingly,  $T_{cn}$  has maximum  $1.93 \times 10^8$  K at  $\rho = 5.62 \times 10^{14} \text{ g cm}^{-3}$  and vanishes at  $\rho = 1.80 \times 10^{15} \text{ g cm}^{-3}$ . The dashed line corresponds to  $T_0 = 6.461 \times 10^9$  K,  $k_1 = 1.961 \text{ fm}^{-1}$ ,  $k_2 = 2.755 \text{ fm}^{-1}$ ,  $k_3 = 1.30 \text{ fm}^{-1}$ . Thus,  $T_{cn}$  has maximum  $3.41 \times 10^8$  K at  $\rho = 4.52 \times 10^{14} \text{ g cm}^{-3}$  and vanishes at  $\rho = 1.78 \times 10^{15} \text{ g cm}^{-3}$ .

The dashed-curve SF has somewhat larger maximum  $T_{cn}$  and appears at earlier cooling stage. As seen from Fig. 1, any mildly strong neutron SF destroys our theoretical explanation of observational data producing pronounced breaks of the cooling curves. It is evident that the weaker SF of neutrons violates theoretical interpretation of older

NSs. It would be impossible to explain rather high observed surface temperature of old PSR 1055–52 and RX J1856–3754 by our NS models with sufficiently strong SF of neutrons (regardless of SF of protons). The NS heat capacity would be strongly reduced, neutrino emission due to Cooper pairing of neutrons would be important, and the NS would be much colder. Our interpretation of all sources in Fig. 1 would not be violated only by a weak neutron SF with maximum  $T_{\text{cn}} < 10^8$  K. This result is in line with low values of  $T_{\text{cn}}$  obtained earlier (Yakovlev et al. 1999) using simplified models of  $T_{\text{cn}}$  constant throughout the NS cores. Note that Yakovlev et al. (1999) were unable to explain rather high values of  $T_s^\infty$  for PSR 1055–52. We can provide such an explanation using NS models with somewhat different EOS and more advanced physics input in the NS crust.

### 3. Summary

We have proposed an interpretation of the observations using a simple model of cooling NSs. The model is consistent with observational data if the proton SF in dense matter is rather strong, with the maximum of  $T_{\text{cp}} \gtrsim 5 \times 10^9$  K at  $\rho \sim (2-3)\rho_0$  but decreases sharply at  $\rho \gtrsim \rho_{\text{D}}$ . On the other hand, the neutron SF must be weak, with the maximum  $T_{\text{cn}} < 10^8$  K. Fixing the density profiles of  $T_{\text{cp}}(\rho)$  and  $T_{\text{cn}}(\rho)$  we can explain the observational data by cooling of NSs with the same EOS and SF properties but with different masses. Our interpretation does not require any reheating mechanism in cooling isolated NSs (see, e.g., Yakovlev et al. 1999, for references).

A strong SF of protons is required to smooth transition from slow to fast cooling with increasing NS mass. Otherwise it would be difficult to explain rather low surface temperatures of the Vela and Geminga pulsars. A weakness of neutron SF is necessary to avoid sharp falls of the NS surface temperatures after onset of neutrino emission due to Cooper pairing of neutrons. Weak neutron SF is in favor of a not too soft EOS in the NS core (softness would mean strong attractive nn interaction and therefore strong neutron pairing). Strong proton SF is in favor of not too large symmetry energy at high densities (too large symmetry energy would mean large proton number density which would suppress proton pairing). On the other hand, the symmetry energy must be not too small to open direct Urca process at  $\rho > \rho_{\text{D}}$ .

The adopted density dependence  $T_{\text{cp}}(\rho)$  is not unique. We could choose different  $T_{\text{cp}}(\rho)$  profiles satisfying the above criteria and interpret observations in the same manner by cooling of NSs with somewhat different masses. Although we have used one particular EOS in the NS core, about the same results would evidently be obtained for a variety of EOSs.

In our model, the colder NSs, Vela and Geminga, are more massive ( $M \sim 1.45 M_\odot$ ), while the hottest RX J0822–43 and warm and old PSR 1055–52 and RX J1856–3754 are the least massive ( $M \sim (1.1-1.3) M_\odot$ ) of all NSs included in the analysis. The mass range obtained is in

good agreement with the well-known range of masses of radio pulsars in binary systems (Thorsett & Chakrabarty 1999). Note that in our model neutrons in the NS cores remain nonsuperfluid for  $t \lesssim 10^6$  yr. Furthermore, massive NSs,  $M \gtrsim 1.5 M_\odot$ , must undergo fast cooling and be cold,  $T_s^\infty \lesssim 3 \times 10^5$  K (the lowest solid curve in Fig. 1). Thus, we could explain the existence of cold middle-aged NSs, if such objects were discovered, as massive NSs. On the other hand, it would be easy to modify the model to avoid prediction of these cold NSs. This can be done by choosing the EOS in the NS core in which  $\rho_{\text{D}}$  is close to  $\rho_{\text{c,max}}$ . Another possibility is to adopt the  $T_{\text{cp}}(\rho)$  profile with  $T_{\text{cp}}(\rho_{\text{c,max}}) \gtrsim (2-3) \times 10^9$  K.

Our model may seem oversimplified because it neglects possible presence of other particles (muons, hyperons, quarks) in the NS cores. However, despite its simplicity, it can explain observations of isolated NSs with only one adjustable parameter – NS mass. We are planning to analyze more complicated models in future publications.

*Acknowledgements.* We are indebted to George Pavlov for very helpful discussions, to Kseniya Levenfish for assistance at the initial stage of this work and for helpful critical remarks, and also to Fred Walter and to the referee, Slava Zavlin, for useful critical remarks. The work was supported partly by RFBR grant No. 99-02-18099 and KBN grant No. 5P03D.020.20.

### References

- Gnedin, O. Y., Yakovlev, D. G., & Potekhin, A. Y. 2001, MNRAS (in press; astro-ph/0012306)
- Flowers, E. G., Ruderman, M., & Sutherland, P.G. 1976, ApJ 205, 541
- Halpern, J. P. & Wang F. Y.-H. 1997, ApJ 477, 905
- Lattimer, J. M., Pethick, C. J., Prakash, M., & Haensel, P. 1991, Phys. Rev. Lett. 66, 2701
- Lyne, A. G., Pritchard, R. S., Graham-Smith, F., & Camilo, F. 1996, Nature 381, 497
- Ögelman, H. 1995, in Lives of Neutron Stars, eds. M. A. Alpar, Ü. Kiziloğlu, J. van Paradjis, NATO ASI Ser. (Kluwer, Dordrecht) p. 101
- Page, D. & Applegate, J. H. 1992, ApJ 394, L17
- Pavlov, G. G., Zavlin, V. E., Aschenbach, B., Trümper, J., & Sanwal, D. 2000, ApJ 531, L53
- Pavlov, G. G., Zavlin, V. E., Sanwal, D., Burwitz, V., & Garmire, G. P. 2001, ApJ 552, L129
- Possenti, A., Mereghetti, S., & Colpi, M., 1996, A&A 313, 565
- Potekhin, A. Y., Chabrier, G., & Yakovlev, D. G. 1997, A&A 323, 415
- Prakash, M., Ainsworth, T. L., & Lattimer, J. M. 1988, Phys. Rev. Lett. 61, 2518
- Thorsett, S. E. & Chakrabarty D. 1999, ApJ 512, 288
- Walter, F. M. 2001, ApJ 549, 433
- Yakovlev, D. G., Levenfish, K. P., & Shibano, Yu. A. 1999, Physics–Uspekhi 42, 737
- Yakovlev, D. G., Kaminker, A. D., Gnedin, O. Y., & Haensel, P. 2001, Phys. Rep. (in press; astro-ph/0012122)
- Zavlin, V. E., Pavlov, G. G., & Trümper, J. 1998, ApJ 525, 959
- Zavlin, V. E. & Pavlov, G. G. 1999, private communication
- Zavlin, V.E., Trümper, J., & Pavlov, G.G. 1999, ApJ 525, 959